Journal of Wind Engineering & Industrial Aerodynamics 179 (2018) 200–214

Contents lists available at ScienceDirect

Journal of Wind Engineering & Industrial Aerodynamics

journal homepage: www.elsevier.com/locate/jweia

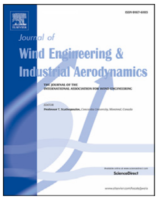

On the onset of vortex shedding past a two-dimensional porous square cylinder

K. Anirudh, S. Dhinakaran [*]

The Centre for Fluid Dynamics, Discipline of Mechanical Engineering, Indian Institute of Technology Indore, Simrol, Indore, 453 552, India

ARTICLE INFO

Keywords:
Darcy-Brinkman-Forccheimer model
Onset of vortex shedding
OpenFOAM
Porous square cylinder

ABSTRACT

Vortex shedding is an interesting phenomenon and a fundamental problem when it comes to flow across bluff bodies. Generation of vortices behind a porous bluff body is further compelling to study. In this paper, a numerical investigation on the onset of vortex shedding behind a porous square cylinder is presented for $41 \leq Re \leq 50$ and the computations are performed for different values of permeability (Darcy number, $Da = 10^{-6} - 10^{-2}$) and porosity ($\varepsilon = 0.629 - 0.993$). Besides, an outlook on unsteady flow across the permeable cylinder is provided for $Re = 50 - 150$. The numerical simulations are performed by modifying pimpleFoam solver of OpenFOAM 4.1 coupled with Darcy-Brinkman-Forchheimer model, using a single domain approach. Current study provides an insight on the influence of permeability on the initiation of vortex shedding behind the porous bluff body. A brief discussion is provided on the jump in flow characteristics, at intermediate values of Darcy number, comparing square with other bluff shapes. Also, a correlation for the frequency of vortex shedding is given in terms of the flow and material parameters. Optimistically, scholars and engineers working on flow control using porous media will benefit from the information presented in this article.

1. Introduction

Flow around porous bluff bodies is seen to buck the trend, owing to its relevance in several technical problems. These studies also provide engineers with a general guideline on how to apply the porous media theory for computational simplification and economy. One can directly simulate a real-time porous media case by simplifying it to a resembling porous bluff body or indirectly, by considering the overall arrangement of individual elements of the system as a single porous object. As an illustration, an outstanding numerical investigation by (Bhattacharyya et al., 2006) on porous circular cylinder can be looked into. The underlying modelling theory advocated by this article was further utilised for diverse applications like marine biological modelling (Khalili et al., 2010), modelling of circulating tumor cell detection (Swaminathan et al., 2013), aerosol respirator design (Zaripov et al., 2016), etc. Another such application of porous media is flow control (Cheung and Melbourne, 1988; Lee and Kim, 1998; Bruneau and Mortazavi, 2008; Bhattacharyya and Singh, 2011; Hasan et al., 2012; Belloli et al., 2014; Liu and Azarpeyvand, 2016; Mimeau et al., 2017) and it has also been attracting researchers recently, due to its affluent flow physics. When the fluid flows across a porous bluff body, at lower values of permeability (Darcy number, Da) and porosity (ε), the permeable body resembles its solid counterpart. However, at higher Da and ε, as more fluid enters the cylinder, distinct variations in flow trends are apparent. This occurrence is used to control the flow i.e. to suppress flow instabilities, where it is a prime concern in slender structures such as chimneys, towers and bridge decks. Amongst various porous bluff cross-sections, square cylinder is the most studied and practically relevant, and is therefore, considered in this study.

A closer rumination of the flow across porous square cylinder can be found in the literature. As stated above, at low values of Da ($\leq 10^{-6}$), almost no fluid enters through the cylinder, which makes it solid-like. But at higher Da ($\geq 10^{-6}$), fluid penetrates through, resulting in an overall reduction in drag coefficient and wake length, for lower Reynolds number (below 40) (Dhinakaran and Ponmozhi, 2011). Two recirculating wakes develop downstream the porous square cylinder in this steady flow regime. Unlike solid cylinder, at higher permeability levels, the wakes are detached from cylinder surface and they exhibit only one separation point along the horizontal axis (Yu et al., 2010). In the unsteady flow regime, at higher Re (above 40) and $Da = 10^{-6}$ (solid cylinder), drag coefficient continues to decrease, however, wake length and the frequency and intensity of vortex shedding increase (Sohankar et al.,

---

[*] Corresponding author.
E-mail address: ssdhinakar@gmail.com (S. Dhinakaran).

https://doi.org/10.1016/j.jweia.2018.03.004
Received 30 August 2017; Received in revised form 6 February 2018; Accepted 4 March 2018

Nomenclature

$\overline{C_p}$	coefficient of pressure, $(p - p_\infty)/(0.5\rho U_\infty^2)$
$\overline{s}$	velocity of fluid in porous region, (ms^{-1})
C_D	coefficient of drag, $D/(0.5\rho U_\infty^2 W)$
C_L	coefficient of lift, $L/(0.5\rho U_\infty^2 W)$
D	drag force acting on the porous cylinder (N)
d_p	diameter of the spherical particle of packed bed (m)
Da	Darcy number, κ/W^2
F	inertial factor, $(1.75/\sqrt{150}) \cdot (1/\varepsilon^{1.5})$
L	lift force acting on the porous cylinder (N)
L_D	non-dimensional distance between rear face of the cylinder and the outflow boundary
P	dimensionless pressure, $p/\left(\rho_f U_\infty^2\right)$
p	pressure of the fluid, (Nm^{-2})
Pr	Prandtl number, ν/α
Re	Reynolds number, $U_\infty W/\nu$
t	dimensional time (s)
U, V	non - dimensional x, y - component of velocity, u/U_∞, v/U_∞
u, v	x, y - component of velocity (ms^{-1})
W	height of the porous cylinder
X, Y	non-dimensional horizontal, vertical distance, x/W, y/W
x, y	horizontal, vertical distance (m)

Greek

Δ	non-dimensional largest grid size
δ	non-dimensional smallest grid size
ε	porosity
κ	permeability of a material (m^2)
μ	dynamic viscosity $(kgm^{-1}s^{-1})$
ρ	density (kgm^{-3})
τ	non-dimensional time, tU_∞/W

Subscript

0	inlet value
∞	far field value
e	effective value
h	high
l	low
m	intermediate
p	particle
rms	root mean square value

1999). At $Da = 10^{-5}$ (near solid cylinder case), the vortex shedding occurs early and lasts longer in terms of Re. With better permeability (higher Da), both the period and intensity of vortex shedding decrease, followed by complete suppression beyond $Da = 10^{-2}$ (Jue, 2004). Moreover, with a larger Da, Re has to be higher before the vortices are shed alternatively (Chen et al., 2008). Porosity variation, for a constant particle diameter, does not affect results much for the same permeability level. On the contrary, for variable particle diameter, results are seen to vary significantly at different values of porosity and Darcy number. It should be noted that this variation succumbs at higher Re (Chen et al., 2009). But, the exact details on the onset of vortex shedding ($Re = 40-50$) and unsteady flow ($Re = 50-150$) around and through a porous square cylinder is nowhere to be found in the open literature.

A jump in drag coefficient at intermediate values of Darcy number (around 10^{-3}) and at $Re > 20$ is already documented for porous circular cylinder (Noymer et al., 1998) (both steady and unsteady regime) and square cylinder (Dhinakaran and Ponmozhi, 2011) (only steady regime). While this jump may exist for bodies with non-streamlined fore-bodies and short aft-bodies, more streamlined porous bodies like trapezoidal (Chen et al., 2009) and diamond cylinders (Rashidi et al., 2014) did not unveil this jump. Description of other flow tendencies at this spike regime is lacking in both steady and particular unsteady regime for porous square cylinder.

Literature on the instigation of vortex shedding in the flow behind solid bluff bodies is in abundance, since the first study on the topic (Jackson, 1987). Henderson, 1995 provide their high resolution computer simulation results for a circular cylinder near the beginning of vortex shedding. They detail the drag curve with proper quantification of viscous drag, pressure drag and base pressure coefficients. The critical Reynolds number (Re_{cr}) for the onset of vortex shedding is reported to be 46 ± 1. Both, the pressure and drag coefficients ($\overline{C}_D$) are seen to decrease up to a certain Re_{cr} value, and then increase with Re uniformly. The rise in drag coefficient value beyond Re_{cr} is credited to jump in pressure drag force (Senthil Kumar and Biswas, 2008). detailed the results of finite-element simulations used to find constants of the Landau equations for flow across a solid circular cylinder. The vortex shedding exists beyond $Re_{cr} = 45.376$ in their analysis at a critical value of Strouhal number, $St = 0.1323$. Sensitive dependency of blockage ratio on the beginning of vortex shedding is also pointed out in their analysis. Sohankar et al., 1995 carried out numerical calculations of vortex shedding past a square cylinder, at $Re = 45$–200 for 5% blockage ratio. Their results suggest that onset of vortex shedding occur between $Re = 50$–55 and beyond this, the flow develops to exhibit well-defined vortex shedding frequency. In a more recent numerical work (Sohankar et al., 1998), arrived at a more accurate value of $Re_{cr} = 51.2 \pm 1$ for the same numerical setup. In an experimental attempt (Sohankar et al., 1997), however, they declared $Re_{cr} = 47 \pm 2$ for practically zero-blockage ratio configuration. It is clear that critical Reynolds number for commencement of vortex shedding increases with blockage ratio. Also, at $\alpha = 45^\circ$ (diamond cylinder), onset occurs at $Re_{cr} = 42 \pm 1$, showing that vortices shed early as inclination angle increases. Sohankar et al., 1999 simulated unsteady, incompressible 2D flow around a solid square cylinder at incidence, at $Re = 45-200$. Influence of blockage ratio and inclination angle on the overall flow behaviour, particularly origination of vortex shedding is stated. They have observed that the flow behaviour at low angles of incidence (particularly at $\alpha \leq 20^\circ$) is distinct from the fully separated flow at higher angles of incidence. At zero angle of incidence, they have reported Re_{cr} to be 51.2 ± 1. Sharma and Eswaran, 2004 presented numerical results which agree with the earlier onset regime (Sohankar et al., 1997, 1999). The mean recirculation length (L_R) and $\overline{C}_D$ are stated to decrease, while St and root mean square value of lift coefficient ($(C_L)_{rms}$), are observed to increase as Re is increased due to higher momentum. Lankadasu and Vengadesan, 2008 studied the influence of a linear shear at inlet on the onset of vortex shedding, and its corresponding effect on mean drag coefficient. A critical Reynolds number of $Re_{cr} = 46 \pm 1$, 43 ± 1 and 39 ± 1 is recorded for shear parameter values of 0, 0.1 and 0.2, respectively. They have noticed that the instigation of vortex shedding is pre-poned and mean drag coefficient decreases as the shear parameter is increased. Knowledge of vortex shedding commencement is also made available for other bluff body shapes recently. Paul et al., 2014 proclaimed $Re_{cr} = 512.5 \pm 0.5$, 231.5 ± 0.5, 87.5 ± 0.5 and 64.5 ± 0.5 for different axis ratio values (ratio of major to minor axes) of 0.1, 0.4, 0.6 and 0.8, respectively for unconfined flow domain. A critical Reynolds number between 69 and 70 was predicted for the flow across a solid semi-circular cylinder by Kumar et al., 2016 for a confined domain (25% blockage ratio). In summary, the flow characteristics differ before and after the onset of vortex shedding significantly, and the same is very sensitive to shear parameter, blockage ratio, axis ratios and inclination of the incoming flow.